



Phase diagram calculation and predication of Au–Pd–Zr ternary system

Jie Yu, Lin-Jing Liu, Shou-Dong Chen,
Jing-Chao Chen*

Received: 21 October 2013 / Revised: 26 March 2014 / Accepted: 6 November 2014 / Published online: 17 December 2014
© The Nonferrous Metals Society of China and Springer-Verlag Berlin Heidelberg 2014

Abstract Au–Pd–Zr ternary alloy phase diagram at 25 °C was calculated by Panda phase calculation software, and the thermodynamic data were based on three binary alloy phase diagrams: Pd–Au, Au–Zr, and Pd–Zr. Five composition points in the ternary phase diagram were selected to predict the precipitation order. One (32Au–32Pd–36Zr) of the five composition points in ternary phase diagram was chosen to verify the correctness of the phase diagram calculation and the precipitation order by scanning electron microscopy (SEM), energy dispersive spectroscopy (EDS), and X-ray diffraction (XRD). The unknown phase in XRD patterns was predicated by EDS and materials studio (MS) software. The experimental results show that there are seven key ternary reactions points and 17 phase regions in all isothermal sections at 25 °C. The thermodynamic process and microstructure for the alloy phase can be described in order according to the vertical section in phase diagram. The phase compositions of the chosen one point are consistent with calculation prediction. The unknown phase in XRD patterns should be Zr_2AuPd by the first principle X-ray simulation.

Keywords Calculated phase diagram; Ternary alloy; Thermodynamic; Phase transformation; Annealing

1 Introduction

Owing to lower elastic modulus, Au–Pd alloys could not withstand higher corrosion and strength. Adding a small amount of alloy elements can improve the alloy's elastic modulus. V, Cr, Fe, Zr, and other elements are often used to improve the mechanical and electrical properties of alloys, and thus get high strength and resistivity [1–4]. As an typical element, Zr is often used to improve the alloy's instability for arc erosion, poor solder wettability, and low catalytic efficiency, but there are few related reports on the phase diagram of Pd–Au–Zr alloy system until now.

The Pd–Au–Zr ternary system consists of three binary systems, Pd–Au, Au–Zr, and Pd–Zr. Okamoto and Masalski [5] studied the Pd–Au binary phase diagram, they found that the Pd–Au binary phase diagram contained liquid, a continuous solid solution phase (Au–Pd), three intermediate phases, Au_3Pd , $AuPd_3$, and the existence of ordered phase $AuPd$ at low temperature. Lomello-Tafin et al. [6, 7] reported seven intermediate compounds, Zr_3Au , Zr_2Au , Zr_5Au_4 , Zr_7Au_{10} , $ZrAu_2$, $ZrAu_3$, and $ZrAu_4$ in the Au–Zr system; however, the structures of Zr_5Au_4 and Zr_7Au_{10} were not determined clearly. They assessed the Au–Zr phase diagram through differential thermal analysis (DTA), X-ray diffraction (XRD), and electron probe microanalysis (EPMA) technique, including the identification of the liquid equilibrium, and found two new intermediate compounds Zr_3Au_2 and $ZrAu$. According to the experimental measurement, Zr_5Au_4 was not an independent compound and $ZrAu$ phase was an intermediate phase with some homogeneous area. Waterstrat et al. [8] used CALPHAD technique to predict the Pd–Zr phase diagram, which was in good agreement with the experimental data. Li et al. [9] used the CALPHAD technique to reassess the Au–Zr phase diagram; the result was in accord with the

J. Yu, S.-D. Chen, J.-C. Chen*
Faculty of Material Science and Engineering, Kunming
University of Science and Technology, Kunming 650093, China
e-mail: chenjingchao@kmust.edu.cn

L.-J. Liu
Mechanical Engineering and Automation Department, Hunan
Biological and Electromechanical Polytechnic,
Changsha 410127, China

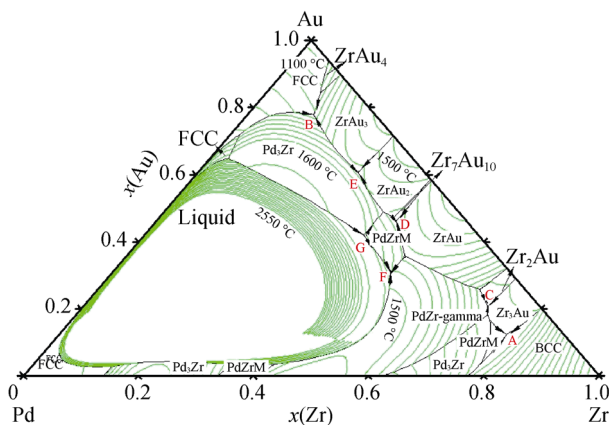


Fig. 1 Calculated liquidus projection of Au–Pd–Zr system

Table 1 Key ternary reactions and temperatures corresponding to Points A–G in Fig. 1

Points	Temperature/ °C	Reactions
A	982.59	Liquid → Zr ₃ Au + PdZrM + BCC
B	1,207.68	Liquid + Pd ₃ Zr → FCC + ZrAu ₃
C	1,024.29	Liquid → PdZr ₂ gamma + Zr ₃ Au + Zr ₂ Au
D	1,365.97	Liquid → PdZrM + ZrAu + Zr ₇ Au ₁₀
E	1,429.33	Liquid → Pd ₃ Zr + ZrAu ₃ + ZrAu ₂
F	1,454.65	Liquid → Liquid + PdZrM + PdZr ₂ gamma
G	1,558.99	Liquid + Pd ₃ Zr → Liquid + PdZrM

experimental data. Guo et al. [10] assessed the Pd–Zr system and set up three sublattice models for order–disorder transformation between Pd–Zr phase and Pd₃Zr phase. The results were in good agreement with the experimental results and the self-consistent thermodynamic interaction parameters were obtained. In this paper, the liquid phase projection and isothermal section for the ternary system were predicted through Panda phase calculation software, and the thermodynamic data were based on the research of Pd–Au, Au–Zr, and Pd–Zr binary phases.

2 Experimental

The phase diagram of the Au–Pd–Zr system was calculated by published thermodynamic descriptions for the constitutive binary systems. The Gibbs energy functions for pure elements were taken from the Science Group Thermodata Europe database [11]. The thermodynamic parameters for Pd–Au, Au–Zr, and Pd–Zr systems from Refs. [5, 9, 10], correspondingly, were directly used in this work.

The raw materials were Au (99.99 wt% spongy), Pd (99.99 % wire), and Zr (99.99 %), and the above metals were melted by GP30-CW7 high-frequency induction

furnace with vacuum degree of 5×10^{-2} Pa, then argon gas was used for protection during melting. After melted to composition, uniformed entirely, the alloys were cooled to room temperature in the furnace and then annealed in 1,100 °C for 72 and 144 h, respectively.

All the samples were metallographically prepared. After etching, optical microscopes (OM, XWJ02) and scanning electron microscope with energy dispersive spectroscopy (SEM–EDS, S-3400N) were used for microscopic appearance analysis. X-ray diffraction (DMAX-RC) was used for the alloy phase analysis, measured by the target of Cu K α , 40 kV/40 mA, scanning angle of 0°–90°. The results of XRD were judged by Jade5.0.

3 Results and discussion

3.1 Calculated phase diagram

As shown in Fig. 1, the highest temperature in liquidus surface is 2,550 °C with the extrapolated liquidus projection of the Au–Pd–Zr ternary system, and the calculated liquidus projection shows a large composition region of liquid immiscibility. The dense liquid isotherms indicate that the three-dimensional map is very steep, resulting in large change of temperature within the alloy of liquid compositions. In the middle phase (near the Au–Pd border), the isotherm distribution is sparser, thus the liquid surface of the alloy in three-dimensional figure is relatively flat, and the temperature changes more slowly with the changing composition.

Seven key ternary reactions are shown in this liquidus projection (A–G). The temperature of a ternary eutectic reaction point (A) close to the binary Pd–Zr is 982.59 °C. This temperature represents the lowest temperature of thermodynamic stability of the liquid phase in this ternary system according to the thermodynamic prediction. The seven key ternary reactions and corresponding temperatures are given in Table 1.

There are 17 phase regions in all isothermal sections at 25 °C as shown in Fig. 2. The alloy is based on Au–Pd matrix and the mole ration of Au to Pd is 1:1, the amount range of Zr is 0–1, the starting point of red line means that the composition is 0.5Au–0.5Pd–0Zr and the end point is 0Au–0Pd–1Zr. The precipitation orders for the five points in red line of Fig. 2 are shown as below according to the vertical section of Fig. 3: Point 1, liquid → Pd₃Zr + liquid → Liquid + Pd₃Zr + ZrAu₂ → ZrAu₂ + ZrAu₃ + Pd₃Zr; Point 2, liquid → Pd₃Zr + liquid → liquid + Pd₃Zr + ZrAu₂ → Pd₃Zr + ZrAu₂ + PdZrM → ZrAu₂ + Pd₃Zr + Zr₇Au₁₀; Point 3, liquid → PdZrM + liquid + liquid → PdZrM + liquid → liquid + ZrAu + PdZrM → ZrAu + PdZrM + Zr₇Au₁₀; Point 4, liquid → PdZrM + liquid + liquid → liquid + PdZrM → ZrAu + PdZrM + Pd₄Zr₃.

Alloy 3 is selected to specify the crystallization process. The process is described in order from 1 to 6 according to the enlarged portion in Fig. 3: 1'–2', liquid → Pd₃Zr; 2'–3', liquid + Pd₃Zr → PdZrM + liquid at 1,558.99 °C, and Pd₃Zr also exists; 3'–4', liquid + Pd₃Zr → PdZrM + ZrAu₂ in 1,403.77 °C, and the system exists three phases (liquid + PdZrM + ZrAu₂); 4'–5', liquid → Zr₇Au₁₀ and PdZrM + ZrAu₂ → Pd₃Zr + Zr₇Au₁₀ at 1,017.89 °C; 5–6, PdZrM + Pd₃Zr + Zr₇Au₁₀ exist. Therefore, the whole solidification process of Alloy 3 is liquid → Pd₃Zr + liquid → liquid + Pd₃Zr + PdZrM → liquid + ZrAu₂ + PdZrM → ZrAu₂ + PdZrM + Zr₇Au₁₀.

3.2 XRD and EDS analysis for experiment phenomena

Verification experiments for Alloy 3 make the calculation more reasonable. As shown in Fig. 4a, the light gray color

organizations are surrounded by deeper gray organizations in the circle section, and the point-like organizations in oval section appear after annealing for 72 h, which are similar to peritectic organization [12]. The precipitation phases show a transitional diffusion state from B to A region as shown in Fig. 4b, indicating that the unfinished reaction (PdZrM + ZrAu₂ → Pd₃Zr + Zr₇Au₁₀ at 1,017.89 °C) continues during annealing time, and the microstructure should be ZrAu₂ + PdZrM + Zr₇Au₁₀ at room temperature.

The EDS analysis for the point-like (oval section) structure for different annealing time shows that the amount of Pd and Au increases, whereas Zr decreases; meanwhile, the microstructure in circle section disappears and that in oval section appears largely and grows up with annealing time of 144 h, as shown in Fig. 5. The

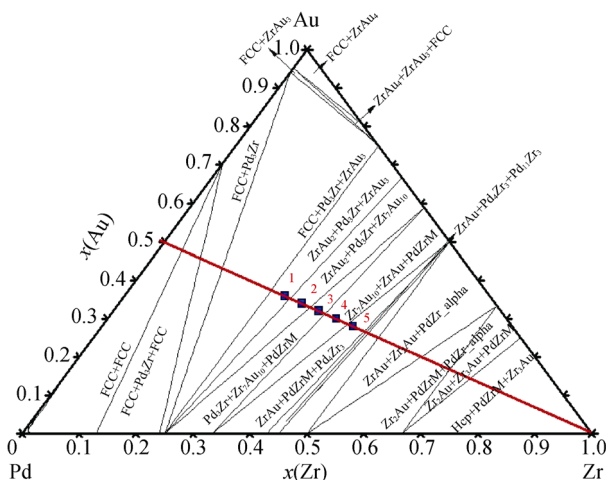


Fig. 2 Calculated isothermal section of Au–Pd–Zr system at 25 °C

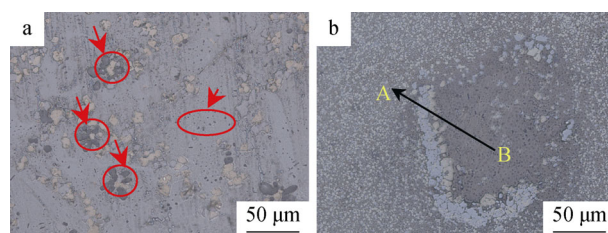


Fig. 4 OM images of Alloy 3 annealing for 72 h: a peritectic microstructure and b peritectic particle

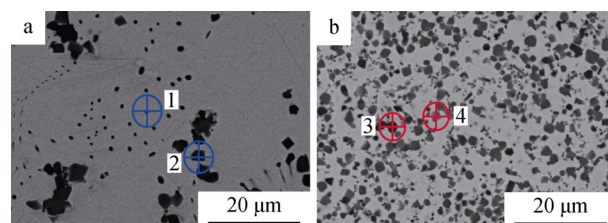


Fig. 5 SEM images of Alloy 3 annealing for a 72 h and b 144 h

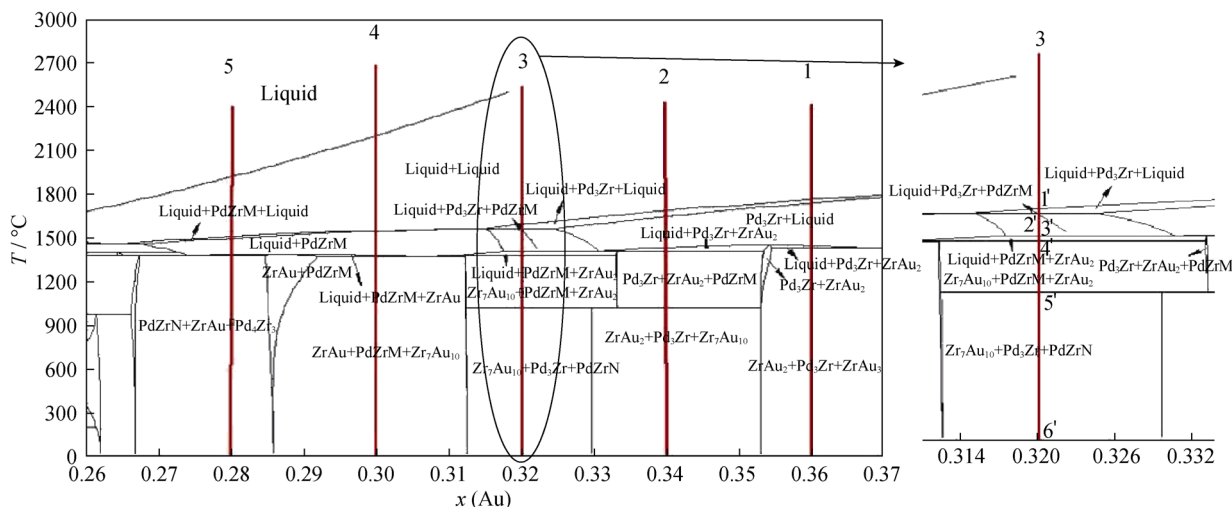


Fig. 3 Vertical section of Au–Pd–Zr system for five corresponding calculated points in Fig. 2 and enlarged portion of Alloy 3

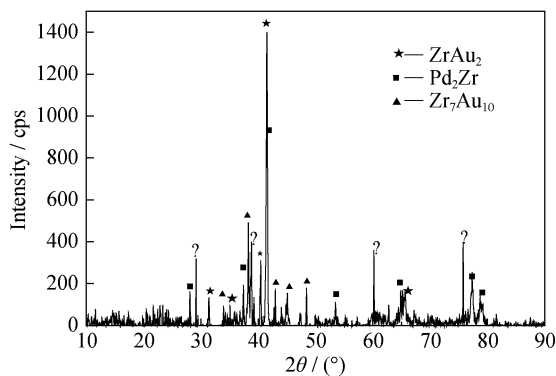


Fig. 6 XRD pattern of annealed Alloy 3

Table 2 EDS results of marked zones in Fig. 5a and b

Zones	x/at%			w/wt%		
	Au	Pd	Zr	Au	Pd	Zr
1	8.49	2.84	88.67	3.00	16.63	80.37
2	12.92	5.64	81.44	24.07	5.67	70.25
3	25.55	18.73	55.71	41.57	16.46	41.97
4	19.67	10.63	69.70	34.09	9.96	55.96

phenomenon can be interpreted that some unbalance phases (may be caused by peritectic reaction: liquid + Pd₃Zr → PdZrM + ZrAu₂ at 1,403.77 °C or PdZrM + ZrAu₂ → Pd₃Zr + Zr₇Au₁₀ at 1,017.89 °C) disappear with long annealing time. The three phases ZrAu₂, PdZrM, and Zr₇Au₁₀ were confirmed by XRD, as shown in Fig. 6. However, there are three stronger diffraction peaks (located at about 30°, 40°, 60°, etc.), and corresponding phases

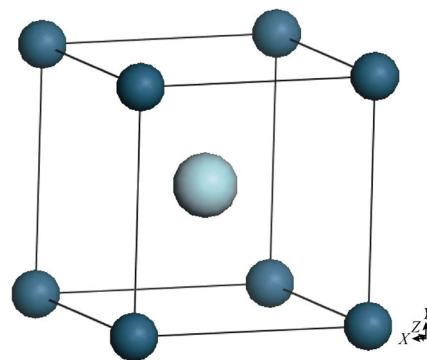


Fig. 7 Simulation model of Zr₂AuPd

cannot be found according to PDF data card; therefore, it maybe ternary compounds.

3.3 Speculated possible ternary compounds

The amount of Zr is higher than those of Pd and Au, thus Zr is considered to be the matrix by EDS analysis in Table 2, and the possible ternary compounds are Zr₂AuPd, Pd₂AuZr, AuPdZr, Zr₂Au₂Pd, and Zr₄Pd₂Au by the ratio of Au:Pd:Zr from EDS analysis. The lattice parameters of possible ternary compounds are listed in Table 3.

The crystal structures of above five phases were created by materials studio (MS) software. The crystal structure model of Zr₂AuPd is shown in Fig. 7, the occupation ratio of Pd atoms and Au atom is 50 % at the (0, 0, 0) position, taken 3 × 3 × 3 super-cell structure. The XRD simulation results show that diffraction peaks for AuPdZr₂ appear at 2θ = 28°, 60°, and the strongest diffraction peak also appears at 2θ = 41° or 42° at the same time, as shown in Fig. 8. It is consistent with the experimental XRD result of

Table 3 Lattice parameters of ternary compounds

Phases	Pearson symbols	Space groups	Lattice parameters/nm	X, Y, Z	Site occupation factor	Prototypes	References
Zr ₂ AuPd	cp2	<i>pm-3m</i>	0.3093	Au(0,0,0)	0.50	AuPdZn ₂	[13]
			0.3093	Pd(0,0,0)	0.50		
			0.3093	Zr(0.50,0.50,0.50)	1.00		
Pd ₂ AuZr	cF4	<i>Fm-3m</i>	0.3978	Au(0,0,0)	0.25	Ag _{0.25} Au _{0.25} Pd _{0.5}	[14]
			0.3978	Pd(0,0,0)	0.50		
			0.3978	Zr(0,0,0)	0.25		
PdAuZr	cF16	<i>Fm-3m</i>	0.6832	Au(0.25,0.25,0.25)	0.50	AuInPdY	[15]
			0.6832	Pd(0.25,0.25,0.25)	0.50		
			0.6832	Zr(0,0,0)	1.00		
Zr ₂ Au ₂ Pd	cF16	<i>Fm-3m</i>	0.6730	Au(0.25,0.25,0.25)	0.50	Au ₂ InZr	[16]
			0.6730	Pd(0,0,0)	1.00		
			0.6730	Zr(0.25,0.25,0.25)	0.50		

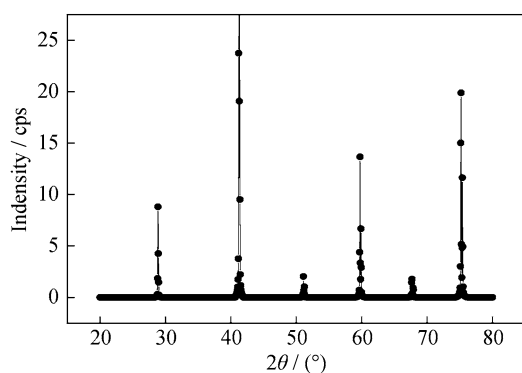


Fig. 8 Simulated XRD pattern for Zr_2AuPd

Alloy 3 in Fig. 6. The simulation results suggest that there is a Zr_2AuPd ternary compound phase.

4 Conclusion

In this article, the method to successfully calculate phase diagram of Au–Pd–Zr ternary system and predication process were reported. The solidification sequence of the alloy 32 % Au–32 % Pd–36 % Zr is liquid \rightarrow Pd₃Zr + liquid \rightarrow liquid + Pd₃Zr + PdZrM \rightarrow liquid + ZrAu₂ + PdZrM \rightarrow ZrAu₂ + PdZrM + Zr₇Au₁₀, and a peritectic reaction liquid + Pd₃Zr \rightarrow PdZrM + ZrAu₂ occurs at 1,403.77 °C. The non-corresponding phase to PDF card for $2\theta = 30^\circ$, 60° and other position in XRD should be Zr_2AuPd . The well agreements for calculation with experiment show that other solidification processes are correct. Our results indicate that the thermal data and the Panda phase calculation software are suitable for directing alloying design and heat treatment.

Acknowledgments This work was financially supported by the National Natural Science Foundation of China (No. 51361036) and the Science Foundation of Kunming University of Science and Technology (No. ZDS2010017C).

References

- [1] Li JY, Xie M, Yang YC, Zhang JM, Chen YT, Liu MM, Wang SB, Hu JQ, Nin P. Effect of Zr, Mo and Y adding on microstructure, mechanical and electrical properties of Au–Pd, Pt–Ir and Pd–Ru systems. *Rare Met Mater Eng.* 2013;10(10):2027.
- [2] Liu HJ, Pan Y, Guan WM, Zhang KH, Yin CP, Du YL. Research progress in superhard transition metal borides. *Chin J Rare Met.* 2013;37(4):633.
- [3] Bai PP, Liu DC, Kong LX, Ma MY, Hu L, Yang B. Drawing method of Ag–Pb–Sn three-dimensional phase diagram. *Chin J Rare Met.* 2013;11(6):930.
- [4] Tang YY, Liao CZ, Meng JL, Zhu JM, Zhu QM, Nong LQ, Liang JL. Phase equilibria in the Fe–Nb–Zr ternary system at 1,200 °C. *Rare Met.* 2013;4(2):201.
- [5] Okamoto H, Massalski TB. The Au–Pd (gold–palladium) system. *Bull Alloy Phase Diagr.* 1985;6(3):229.
- [6] Lomello-Tafin M, Galez P, Feschotte P, Kuntz JJ, Jorda JL, Gachon JC. Enthalpies of formation of Zr–Au compounds determined by direct reaction calorimetry. *J Alloy Compd.* 1998;267:142.
- [7] Lomello-Tafin M, Galez P, Gachon JC, Feschotte P, Jorda JL. The Zr–Au system. *J Alloy Compd.* 1997;257:215.
- [8] Waterstrat RM, Shapiro A, Jeremie A. The palladium–zirconium phase diagram. *J Alloy Compd.* 1999;290:63.
- [9] Li ZH, Jin ZP, Liu HS. Thermodynamic assessment of Au–Zr system. *J Cent South Univ Technol.* 2003;10(2):94.
- [10] Guo CP, Du ZM, Li CR. Thermodynamic modeling of the Pd–Zr system. *Comput Coupling Phase Diagr Thermochem.* 2006;30:482.
- [11] Saunders N, Miodownik AP. In: Robert W, editor. *A Comprehensive Guide, vol. 7. CALPHAD—Calculation of Phase Diagrams.* Cambridge: University of Cambridge Press; 1998. 7.
- [12] Meng W. *Microstructure and Phase Selection in the Unidirectional Solidification of Zn–Cu Peritectic Alloy.* Xi'an: Northwestern Polytechnical University; 2002. 22.
- [13] Krompholz K, Weiss A. X-ray study of the quasibinary system AuZn–PdZn. *J Less-Common Met.* 1976;50(2):213.
- [14] Venudhar YC, Iyengar L, Rao KV. X-ray determination of the effect of temperature on the coefficients of thermal expansion of Pd–Ag–Au alloys. *J Less-Common Met.* 1978;58:55.
- [15] Wernick JH, Hull GW, Geballe TH, Bernardini JE. Superconductivity in ternary Heusler intermetallic compounds. *Mater Lett.* 1983;1(2):90.
- [16] Marazza R, Ferro R, Rambaldi G. Some phases in ternary alloys of titanium, zirconium, and hafnium with an MgAgAs or AlCu₂Mn structure. *J Less-Common Met.* 1975;39:341.